Hindawi
Geofluids
Volume 2022, Article ID 9396616, 12 pages
https://doi.org/10.1155/2022/9396616

Research Article

Error Analysis and Numeric Simulation Research of Parallel Seismic Method

Chao Lin,[1] **Cheng-Lin Zhang**,[1] **Li Rao**,[1] **Chuang Yang**,[1] **Bin An**,[2] **Bao–Feng Zhao**,[2] **Tao Zhan**,[3] **and Xian-Jun Tan**[4]

[1]*Physical Science and Technology College, Yichun University, Yichun 336000 Jiangxi, China*
[2]*The 2nd Engineering Co., Ltd. of China Railway Tunnel Group, Sanhe, 065201 Hebei, China*
[3]*Nanchang Metro Group Co., Ltd., Nanchang 330000 Jiangxi, China*
[4]*Institute of Rock and Soil Mechanics, Chinese Academy of Sciences, Wuhan, Hubei 430000, China*

Correspondence should be addressed to Li Rao; raoli-ycu@hotmail.com

Received 14 April 2022; Revised 21 July 2022; Accepted 25 July 2022; Published 12 August 2022

Academic Editor: Di Feng

The parallel seismic method is an effective method to detect the length of pile. In the paper, based on the ray theory of Snell's law, the two methods of determining the pile length by the first transmission P-wave in the side hole are discussed and modified. The error influencing factors of both two methods are then analysed. Finally, the finite element software ABAQUS was used to simulate the inspection of pile foundations by the parallel seismic method. The numerical simulation results were compared with the results of the error calculation theory to verify the applicability of the error calculation theory. The error calculation theory was then tested and applied in an engineering example. The results show that (1) in order to reduce errors, unreasonable data points need to be removed when fitting the inspection data points and (2) the larger the pile slenderness ratio, the smaller the distance between the side holes and the pile, and the more accurate the pile length results obtained.

1. Introduction

For existing buildings with incomplete original design and construction information, it is necessary to carry out on-site tests on the foundation depth or pile length and the pile body quality when strengthening and renovating or assessing the remaining service life in order to extrapolate the existing load-bearing capacity of the foundation; for buildings that have been built and used for a short time, there will also be the issue of testing the length and quality of such foundation piles that have been connected to the superstructure when their foundation settlement appears abnormally large, or when the quality of their pile foundation is in doubt during the construction of the superstructure.

For piles in newly built projects, as the tops of the piles are exposed, the more simple and convenient method of sonic transmission, core drilling method, and low strain reflected wave method can be used to test the integrity of the piles [1]. However, for the existing building foundation piles, where the top of the pile is connected to the superstructure, it is difficult to accurately detect the pile length and pile quality by conventional testing methods. Parallel seismic method is an effective means of detecting the length of existing building pile foundations, which has started to emerge in recent years [2–4], and its related theoretical research has also been steadily developing. Liao et al. [5] proposed an estimate method to derive the depth of pile foundations through the intersection of 2 fitted straight lines by the means of Snell's law; Huang and Chen [6, 7] established a three-dimensional finite element model of the pile-soil system and analysed the application of this method in cement mixing piles; Chen and Zhao [8] established a simplified model of the first to P-wave transmission path under the homogeneous foundation and thus modified the evaluation method of the depth of existing pile foundations. Subsequently, Du et al. [9] further verified the reasonableness of the simplified model proposed by Chen and Zhao [8] through finite element simulation analysis. Based on the three-dimensional

finite element model, Zhang et al. [10–12] investigated the effect of different excitation methods on the test results of parallel seismic method; Du et al. [13] proposed an improved parallel seismic test method to detect the unknown length and integrity of piles and derived an analytical solution of the t–d relationship for the initial arrival of PS waves under homogeneous and stratified soil conditions. Rashidyan et al. [14, 15] used the parallel seismic wave method to detect the depth of wooden bridge foundations and investigated the effect of striking method and foundation stiffness on the detection results. Huang and Ni [16] found that the pile length estimated by the PS method increased with the distance of the side hole to the pile, but this error could be reduced by applying a length correction factor.

There are a variety of factors that can affect the results of pile testing. Yuan et al. [17] present a method of visualizing the displacement field of the soil around the laterally loaded pile by using transparent soil technology. Bai et al. [18] believe that the changes in the stress states are closely related to soil particle rearrangement and the transitions between different matter phases and derived a generalized effective stress principle. Yuan et al. [19] investigated the role of glass fibers and liquid-modified polyvinyl alcohol polymers in reinforcement of granite residual soils. Bai et al. [20] employed the smoothed particle hydrodynamics (SPH) method to simulate the heat transfer process in porous media at the pore scale and proposed a concise method to produce unsaturated media by simulating the wetting process in dry media. Yuan et al. [21] carried out analyzing the mechanical and deformational behavior of both the material of the laterally loaded piles and soil with groundwater level as a variable.

How to analyse the pile length and pile body quality information from the measured depth-wave-time graph and how to improve the accuracy of the analytical solution require further in-depth study. This research team has carried out some preliminary research work related to concrete quality testing and loading damage in pile foundations [22]. Starting from the transfer law of stress waves in the pile body and soil, this article analyses the pile length information through the measured depth-wave-time graph to improve the accuracy of the analysis, focuses on the sources of error through the test judgment method to verify the validity, validates the theory through the finite element model, and verifies it in the practical engineering applications.

2. Theory of Parallel Seismic Method

Parallel seismic method utilizes the refraction waves carrying information to determine the pile length. A compression wave (P-wave) or shear wave (S-wave) is generated by striking the pile vertically or horizontally with a hand hammer on the top surface (or superstructure such as a bearing or pile cap attached to the top of the pile). The stress wave propagates along the pile body downwards, as shown in Figure 1, and encounters the surrounding soil layer for transmission. A sensor is placed in a hole predrilled next to the pile to receive the transmitted wave signal, from which wave times at different depths are read and from which the first arrival time-depth relationship graph is plotted. When the sensor is below the bottom of the pile, the wave velocity will change and an inflection point will be shown on the time-depth diagram. Therefore, the length of the pile can be deduced from the position in the graph where the slope of the line changes. Additionally, the wave velocities obtained from the slope of the straight line above and below the time-depth diagram can be used to analyse the properties of the pile body material and the pile bottom soil, respectively.

Currently, there are two main methods for determining the depth of the pile in the relevant scientific and technical literature at home and abroad, as shown in Figure 2.

Method 1 is to first fit the upper and lower regions of the time-depth relationship diagram into a straight line (L_1 and L_2) and then treat the depth of their intersection point as the depth of the pile bottom (Z in the figure).

Method 2 is to make a parallel line to the line L_1 through the coordinate origin (0,0) to obtain the line $L_1{}'$ and then treat the depth of the intersection of the line $L_1{}'$ and the line L_2 as the depth of the pile bottom (Z' in the figure).

It has been suggested that the slopes of the upper and lower lines about the time axis are the P-wave velocities of the pile body and the soil below the pile bottom, respectively. For the same test data, it is clear that the depth to the bottom of the pile determined by method 1 is generally greater than that of method 2. Whether the depth to the bottom of the pile can be accurately determined by the straight line intersection method requires more research.

3. Analysis of Stress Wave Transmission Law

3.1. Theoretical Formula for Determining Pile Length. Shu-Tao Liao et al. carried out the theoretical analysis of the transfer of stress waves, on the basis of which this paper further discusses the theoretical error in the method of pile length determination and considers the error caused by the tilt factor of the side hole. Suppose there is a pile partially or completely buried in the soil, as shown in Figure 3, with the pile diameter r, the total pile length L, the pile length above ground level L_A, the distance D from the side hole to the pile body, and the inclination angle α (assuming the side hole is only inclined to one direction). When the external excitation force acts right in the centre of the pile top, the excitation force is assumed to be a point source as the contact area is small relative to the pile body interface. The signals received in the side hole can be separated into two groups, signal group 1 above the bottom of the pile and signal group 2 below the bottom of the pile. The distance from signal B_1 (signal group 1) to the top of the pile is denoted by H_1, and the distance from signal B_n (signal group 2) to the top of the pile is denoted by H_n.

According to the wave transmission law, the stress wave starts from the top of the pile O, passes through the lateral point A_1 of the pile and finally reaches the point B_1. The propagation distance of stress wave $O \longrightarrow A_1 \longrightarrow B_1$ is denoted by S_1. The propagation velocities of the stress wave in the pile and the soil are V_1 and V_2, respectively. The propagation of the stress wave at the intersection of the pile

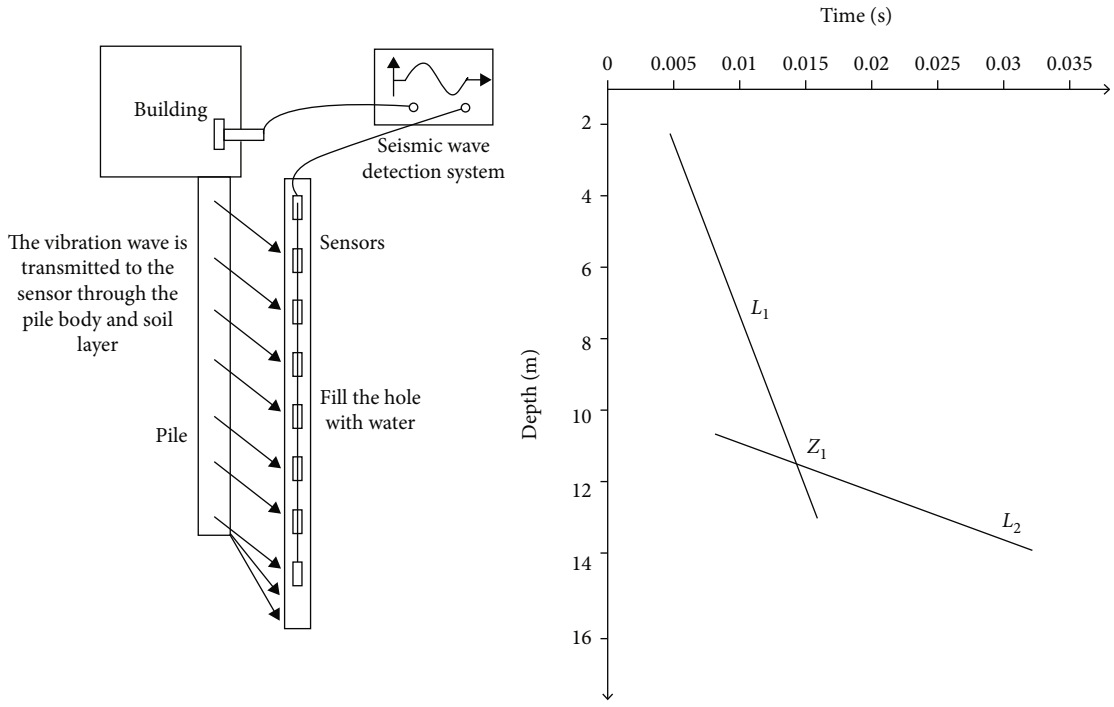

Figure 1: Schematic diagram of the principle of parallel seismic method.

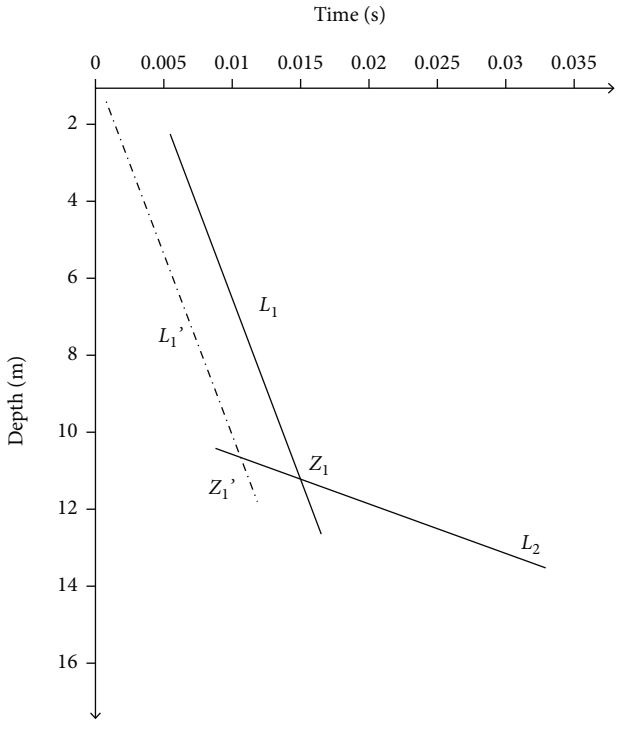

Figure 2: Schematic diagram of the pile bottom depth determination method.

body and the soil should be in accordance with Snell's law, which means

$$\sin \frac{\theta_1}{V_1} = \sin \frac{\theta_2}{V_2}. \tag{1}$$

In the above formula, θ_1 and θ_2 are the refraction angles of the stress wave in the pile medium and soil medium, respectively.

The shortest distance D_a from inspection point B_1 of the side hole to the side of the pile is given by

$$D_\alpha = D + (H_1 - L_A) \tan \alpha. \tag{2}$$

Then, there is

$$\begin{aligned} S_1 &= \sqrt{(H_1 - X)^2 + r^2} + D_\alpha \sec \theta_2 \\ &= (H_1 - X)\sqrt{1 + \left(\frac{r}{H_1 - X}\right)^2} + D_\alpha \sec \theta_2. \end{aligned} \tag{3}$$

In formula (3),

$$X = D_\alpha \cdot \tan \theta_2, \tag{4}$$

$$\theta_2 = \sin^{-1}\left(\sin \theta_1 \cdot \frac{V_2}{V_1}\right) \approx \sin^{-1}\left(\frac{V_2}{V_1}\right). \tag{5}$$

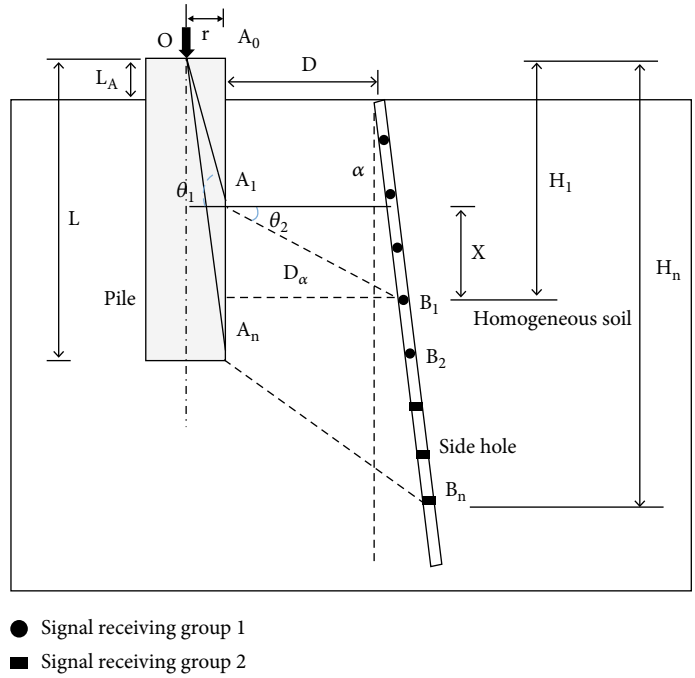

Figure 3: Schematic diagram of the stress wave transmission law.

Then, the total time for the P-wave to travel the distance S_1 to bottom point B_1 is given by

$$T_1 = \frac{(H_1 - X)\sqrt{1 + (r/(H_1 - X))^2}}{V_1} + \frac{D_\alpha \sec\theta_2}{V_2}. \quad (6)$$

The related relationship between P-wave arrival time and depth is shown in Figure 2. L_1 is the signal reception point above the bottom of the pile, and the time formula of L_1 is

$$L_1 : T = \frac{(H - X)\sqrt{1 + (r/(H - X))^2}}{V_1} + \frac{D_\alpha \sec\theta_2}{V_2}. \quad (7)$$

Similarly, assuming that H_n is the distance from the signal reception point B_n (signal group 2) to the top of the pile, the stress wave transmission distance S_n is $O \longrightarrow A_n \longrightarrow B_n$, which is given by

$$S_n = \sqrt{L^2 + r^2} + \sqrt{D_\alpha^2 + (H_n - L)^2} = L\sqrt{1 + \left(\frac{r}{L}\right)^2} + (H_n - L)\sqrt{1 + \left(\frac{D_\alpha}{H_n - L}\right)^2}. \quad (8)$$

Therefore, the propagation time of the distance S_n is

$$T_n = \frac{L\sqrt{1 + (r/L)^2}}{V_1} + \frac{(H_n - L)\sqrt{1 + (D_\alpha/(H_n - L))^2}}{V_2}. \quad (9)$$

Time formula of L_2 in Figure 2 is given by

$$L_2 : T = \frac{L\sqrt{1 + (r/L)^2}}{V_1} + \frac{(H - L)\sqrt{1 + (D_\alpha/(H - L))^2}}{V_2}. \quad (10)$$

The depth of the signal reception point at the intersection of L_1 and L_2 can be obtained by combining equations (7) and (10) as follows:

$$\begin{cases} L_1 : T = \dfrac{(H - X)\sqrt{1 + (r/(H - X))^2}}{V_1} + \dfrac{D_\alpha \sec\theta_2}{V_2}, \\ L_2 : T = \dfrac{L\sqrt{1 + (r/L)^2}}{V_1} + \dfrac{(H - L)\sqrt{1 + (D_\alpha/(H - L))^2}}{V_2}. \end{cases} \quad (11)$$

3.2. Error Analysis of Pile Lengths Determined by Method 1

3.2.1. Discussion of L_1. When $(H - X) >> r$ and $\sqrt{1 + (r/(H - X))^2} \approx 1$, the equation for L_1 can be simplified to a linear equation as follows:

$$L_1 : T = \frac{(H - X)}{V_1} + \frac{D_\alpha \sec\theta_2}{V_2}. \quad (12)$$

For the side hole test point near the ground, L_1 is the curve equation at this point as the condition $(H - X) >> r$ does not hold. Assuming $r = 1$, $L_A = 0.5$, $\alpha = 0°$, $D = 1$, $V_1 = 4000$, and $V_2 = 1000$, the error curve is obtained as shown in Figure 4.

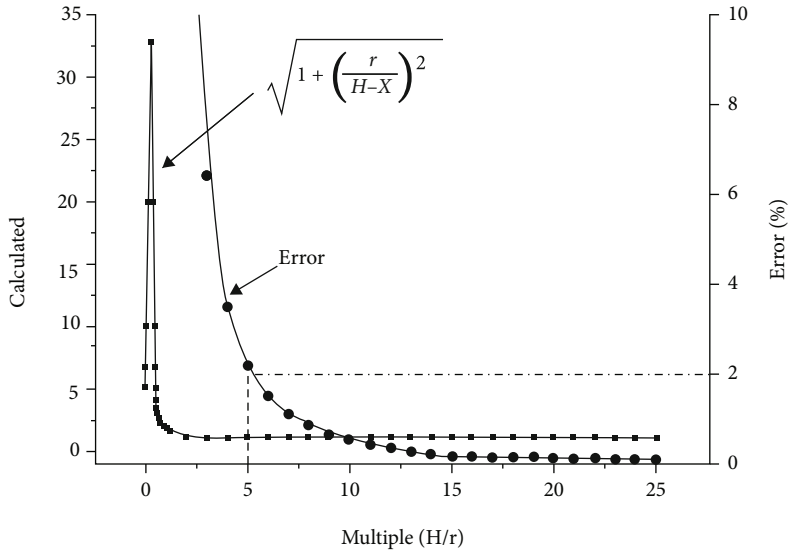

Figure 4: Simplify item error curve.

From Figure 4, it can be seen that the error is already less than 2% when $H \geq 5r$. Also the fitting of a straight line L_1 from the test data points in Figure 2 does not cause too much error.

3.2.2. Discussion of L_2. When $L >> r$, $(H - L) >> D_\alpha$, and $\sqrt{1 + (D_\alpha/(H-L))^2} \approx 1$, the equation for L_2 can be simplified to a linear equation as follows:

$$L_2 : T = \frac{L}{V_1} + \frac{(H-L)}{V_2}. \tag{13}$$

For the side hole test point near the pile bottom, the equation simplification condition does not hold. The error is calculated to be less than 2% when $H - L \geq 5D_a$. Therefore, the fitting of L_2 straight line should be made with the test data points far away from the pile bottom.

3.2.3. Error of Method 1. After simplification, both L_1 and L_2 are straight lines. The intersection of these two straight lines, Z_1, is the depth of the pile bottom, H_p, as determined by method 1. So the formula of H_p is obtained as follows:

$$H_p = L + \frac{V_1}{V_1 - V_2} D_\alpha \sec\theta_2 - \frac{V_2}{V_1 - V_2} X. \tag{14}$$

The actual pile length L can be derived from the above equation:

$$L = H_p - \left(\frac{V_1}{V_1 - V_2} D_\alpha \sec\theta_2 - \frac{V_2}{V_1 - V_2} X\right). \tag{15}$$

In the equation above, $(V_1/(V_1 - V_2)D_\alpha \sec\theta_2 - V_2/(V_1 - V_2)X)$ is defined as the correction factor for the depth of the pile bottom determined by method 1. The more slender the pile to be tested and the smaller the side hole distance, the more accurate the test result will be.

3.2.4. Field Operation Errors due to the Tilted Side Hole. In the field inspection, a time-depth diagram can be plotted through method 1 based on the inspection data. When the actual side hole is inclined at an angle α and the plotted inspection depth is determined as if the side hole were not inclined, the intersection depth value in the plotted time-depth diagram is larger than the depth value calculated by equation (13), as shown in Figure 5. Also in the field site inspection, the depth of the test point is calculated from the ground level, ignoring the height of the pile foundations above the ground level L_A. Combining the above factors, the intersection depth obtained by method 1 plotting has the following conversion relationship with the theoretically calculated intersection depth:

$$H_p = H_{p,\text{inclined}} \times \cos\alpha + L_A, \tag{16}$$

where H_p is the theoretical intersection depth and $H_{p,\text{inclined}}$ is the actual intersection depth obtained by plotting through method 1.

3.3. Error Analysis of Pile Lengths Determined by Method 2. In method 2, the line L_1' is obtained by translating the straight line L_1 along the time axis to the origin of the coordinates in the time-depth diagram. And formula (11) can be transformed into

$$L_1' : T = \frac{H(1 - \tan a)}{V_1} + \frac{H \tan\alpha \sec\theta_2}{V_2}. \tag{17}$$

When equations (13) and (17) are combined, the depth of point Z_1', the intersection of line L_1' with line L_2, can be obtained. The depth of point Z_1' determined through method 2 is the depth of the pile bottom H_p'.

$$H_p' = \frac{L(V_2 - V_1)}{V_2(1 - \tan\alpha) + V_1(\tan\alpha \sec\theta_2 - 1)}, \tag{18}$$

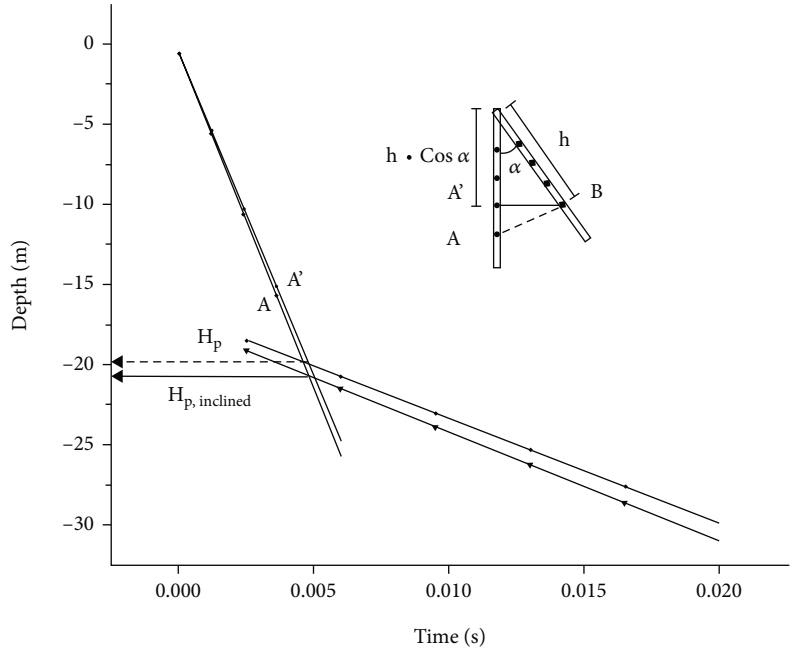

Figure 5: The schematic diagram of field operation errors due to tilted side holes.

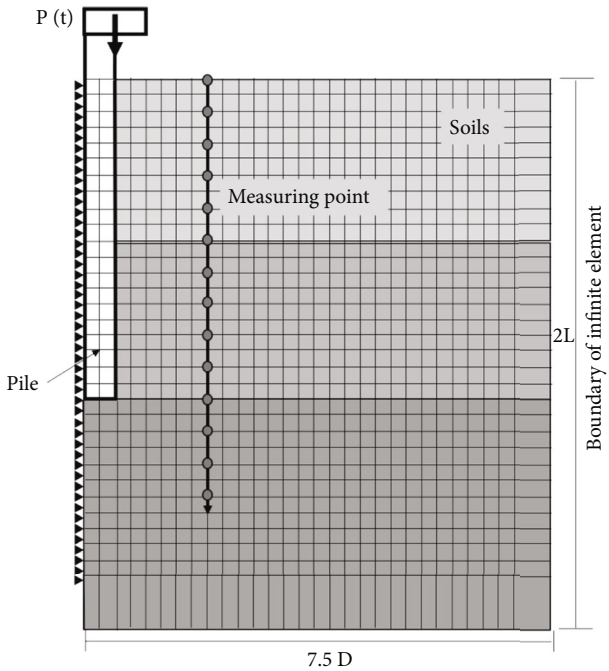

Figure 6: Schematic diagram of the finite element mesh for pile foundation inspection by parallel seismic method.

$$L = H_p'\left(\frac{V_2(1-\tan\alpha)+V_1(\tan\alpha\sec\theta_2-1)}{V_2-V_1}\right). \quad (19)$$

L is defined as the correction factor for the depth of the pile bottom determined through method 2. When $\alpha = 0$, $L = H_p{}'$. This shows that the pile bottom depth determined through method 2 is correct.

4. Finite Element Simulation Analysis and Verification

4.1. Model and Parameters. In recent years, the commercial software ABAQUS has been well used in the numerical simulation of underground engineering [23]. Therefore, we used ABAQUS to build a finite element model to numerically simulate the pile foundation inspection process. A reasonable artificial boundary was set to simulate and analyse the time-depth relationship between the first and P-waves in the parallel seismic wave signal. In the finite element model, the pile diameter D is taken as 1 m and the pile length L is taken as 20 m. After trial calculations, the following grid areas were selected: 7.5 times the pile diameter in the horizontal radial direction, 2 times the pile length in the vertical direction, and the side holes were arranged in the range of 0-5 m on the pile side. CAX4R cells were used for the finite elements and CINX4 cells were used for the boundary infinite elements [5, 6]. Based on symmetry, half of the model was taken along the centreline of the hammer load range for analysis, as shown in Figure 6.

In order to obtain a clear transmission waveform, both the pile and the soil are simplified to a homogeneous linear elastic material in the analysis. For a normal section of the pile, the density is taken as 2300 kg/m^3 with the elasticity modulus of 33.1 GPa and the Poisson's ratio of 0.2. For homogeneous soils, the density is taken as 1900 kg/m^3 with the elasticity modulus of 0.213 GPa and the Poisson's ratio of 0.4. The corresponding wave velocities calculated from the above material properties are shown in Table 1.

The P-wave is the fastest, the S-wave is slightly slower, and the R-wave is the slowest. The monitoring point of the side hole is first stimulated by the P-wave, followed by the S-wave and R-wave. P-wave masses move vertically at a

Table 1: Pile-soil parameters.

Material	Density ρ (kg/m^3)	Elasticity modulus (GPa)	Poisson ratio	P-wave speed (m/s)	S-wave speed (m/s)
Pile shaft	2300	33.1	0.2	3998.79	2448.75
Homogeneous soils	1900	0.213	0.4	490.13	200.09

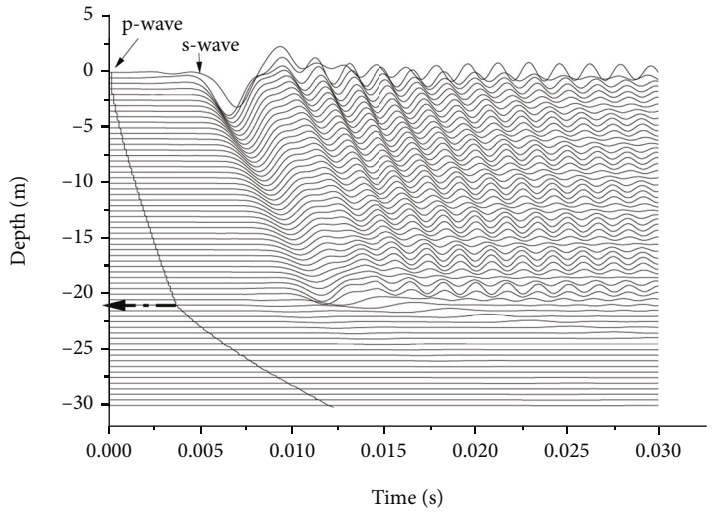

Figure 7: Waveform combination time-depth diagram.

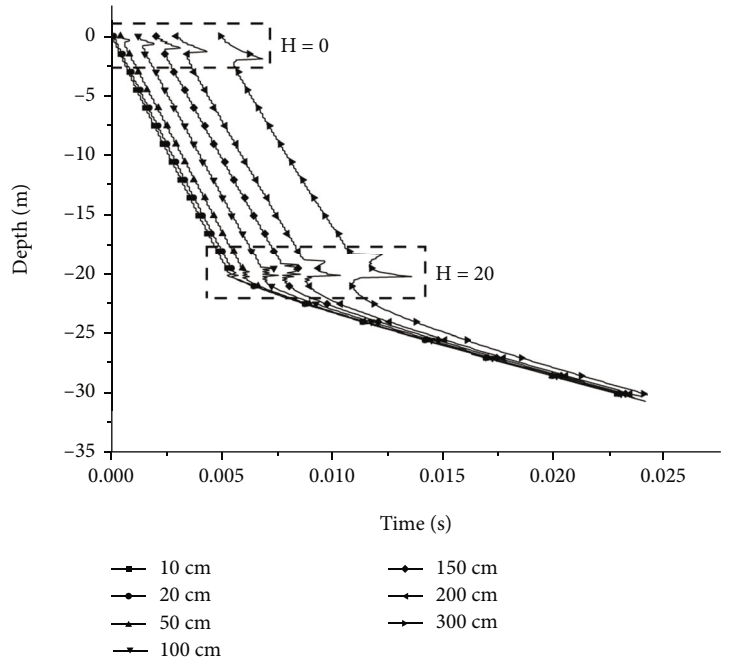

Figure 8: Time-depth comparison for different hole distance.

small speed, decay quickly, and take up a small amount of excitation energy. For the plasmas at a distance from the excitation point, the excitation velocity is mainly influenced by the slower R- and S-waves. Theoretically, the large amplitude of the S-wave plasmas makes the S-wave easier to be identified in the waveform diagram, but it is still difficult to judge the waveform arrival time due to the influence of waveform superposition. A line can be formed by connecting the time points at which the P-waveform starts. The depth corresponding to the turning point of the line is the

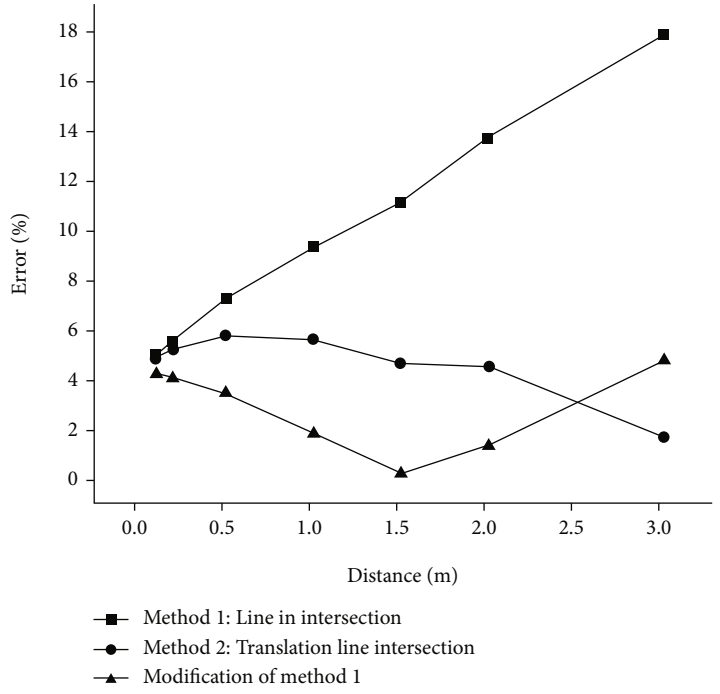

Figure 9: Comparison of the error-side hole distance for different methods of predicting pile bottom depth.

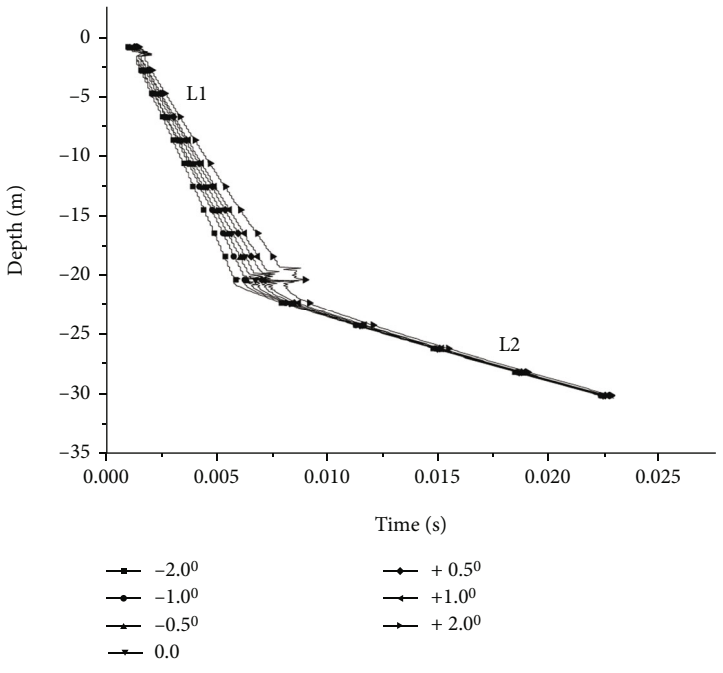

Figure 10: Time-depth diagram under the inclination of the side hole.

depth of the pile bottom, as shown by the arrow at the fold in Figure 7.

4.2. Analysis of the Effect of Distance from the Side Hole. The effect of the side hole distance on the pile length test results was assessed through simulation analysis of a finite element model. The parameters of the finite element model were taken as follows: the distance between the side hole and the edge of the pile $D = 0.1$ m, 0.2 m, 0.5 m, 1 m, 1.5 m, 2.0 m, and 3.0 m in that order; the inclination angle of the side hole $a = 0$; the distance of the vertical excitation point from the ground is 0.5 m; no defects in the pile body; homogeneous soil quality; and the rest of the parameters are the same as before.

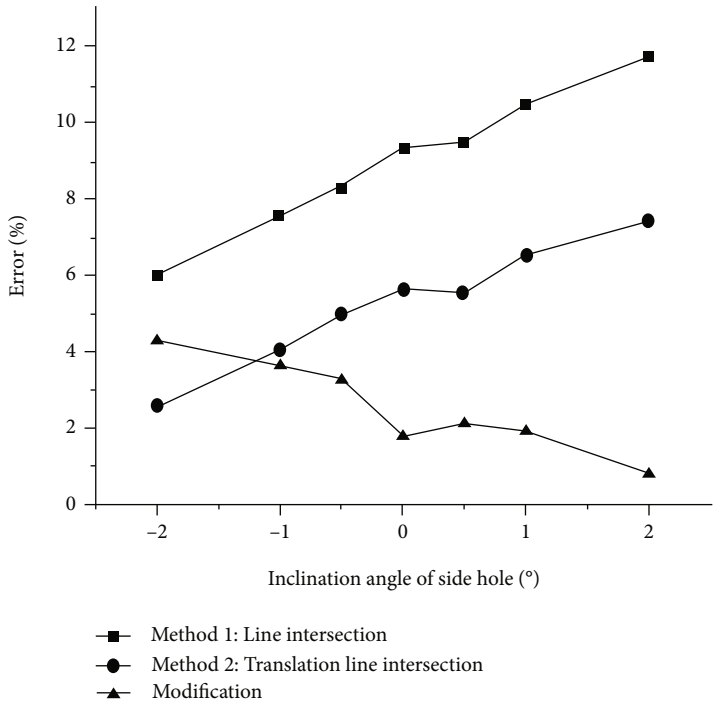

Figure 11: Comparison of the error-side hole inclination for different methods of predicting pile bottom depth.

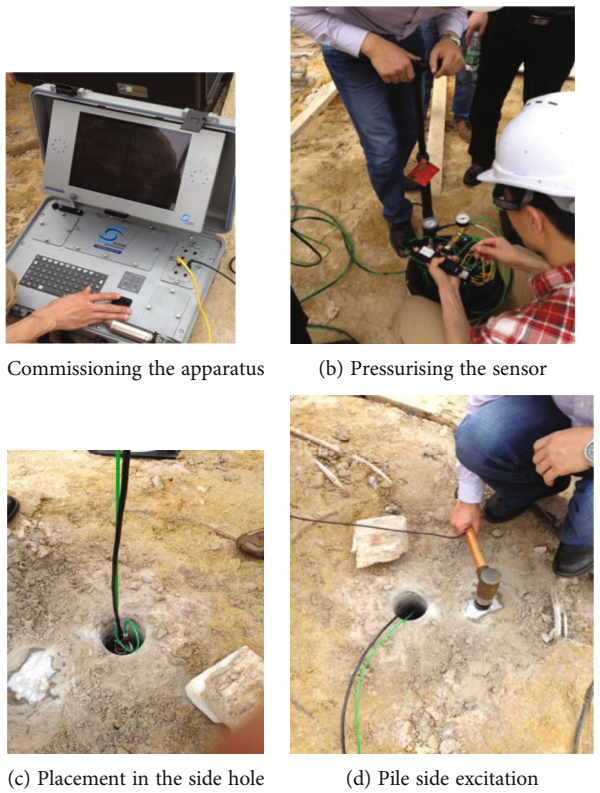

(a) Commissioning the apparatus (b) Pressurising the sensor

(c) Placement in the side hole (d) Pile side excitation

Figure 12: Parallel seismic wave method field testing process.

As shown in Figure 8, the depth of the curve turning point increases as the distance between the side borehole and the pile side increases. Near depth $H = 0$, the data points are distributed in a curved line, which does not conform to the assumption of a straight line L_1. Near the depth $H = 20$ m, the data points are curved and the curve becomes full as the

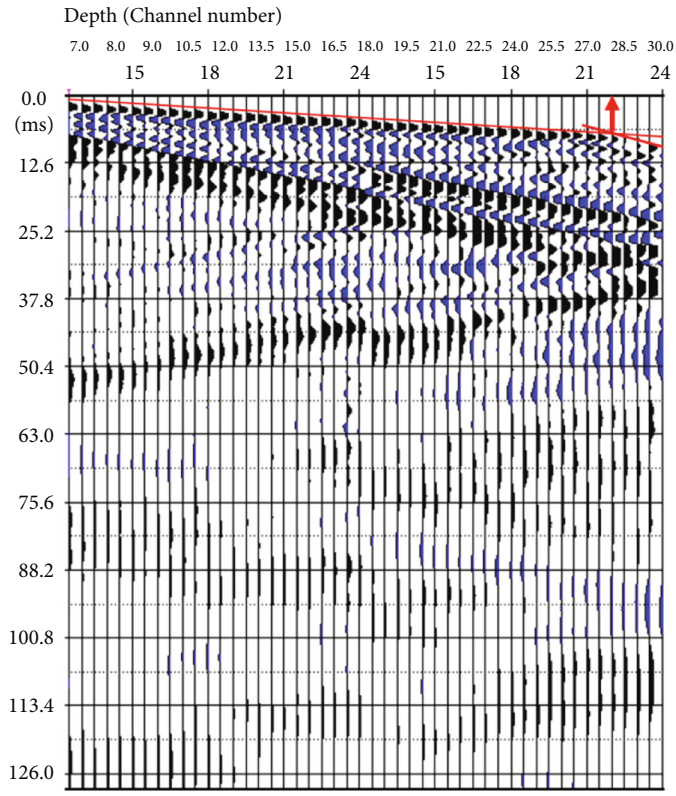

Figure 13: Waveform diagram.

distance D increases, which does not conform to the assumption of straight line L_2. The results of the numerical simulations are in accordance with the aforementioned theoretical analysis.

By comparing method 1 and method 2 with the theoretical correction values, as shown in Figure 9, it can be found that the error of method 1 increases with the increase of the side hole distance, while method 2 can better eliminate the influence of the error caused by the side hole distance through the use of translating straight lines, and the correction effect of the correction method is close to that of method 2.

4.3. Analysis of the Influence of the Side Hole Inclination. The influence of the side hole inclination on test results was assessed through simulation analysis of a finite element model. The parameters of the finite element model were taken as follows: inclination angles of the side hole taken as 0, ±0.50, ±10, and ±20 in that order; the distance of the side hole is 1 m; no defects in the pile body; and homogeneous soil quality.

Figure 10 shows the final simulation results. It can be seen from the figure that the direction of the side hole inclination is the same as the direction of the data point offset and that the side hole inclination has a greater effect on the data point distribution of straight line L_1 and almost no effect on straight line L_2, which is consistent with the results of the previous discussion on straight line L_1 and straight line L_2.

As shown in Figure 11, the error caused by the angle of inclination of the side hole cannot be eliminated. The error of the inclination correction value decreases as the inclination angle increases. The reduction in the error of the inclination correction value better reflects the actual pile bottom depth.

5. Engineering Measurements

There is a filling pile with a diameter of 800 mm and a pile length of 27 m located in a saturated clay layer at a site in Huadu District, Guangzhou. The field pile length inspection was carried out with a DAQlink III distributed seismometer manufactured by Seismic Source, USA. During the inspection process, the pile inclination angle $\alpha = 0$ and the distance between the side hole and the inspection pile $D = 1.0$ m. Figure 12 shows the inspection process in the field.

The waveform diagram was plotted for the signals received at each depth point, with the vertical coordinate being the sampling time and the horizontal coordinate being the depth of each checkpoint, as shown in Figure 13. Based on the aforementioned method 1, the pile length H_p was estimated to be 28.0 m.

The correction volume was used to correct the pile length test results. In China, the one-dimensional P-wave velocity of common concrete piles is 3800~4200 m/s, and the common saturated foundation soil wave velocity is 1300~1700 m/s. Taking the pile wave velocity $V_1 = 4000$ m/s and the soil wave velocity $V_2 = 1500$ m/s, then the following is derived:

$$X = D\tan\theta_2 = D\tan\left(\sin^{-1}\frac{V_2}{V_1}\right) = 1.0\times\tan\left(\sin^{-1}\frac{1500}{4000}\right) = 0.3844, \tag{20}$$

$$L = H_p - \left(\frac{V_1}{V_1 - V_2}D\sec\theta_2 - \frac{V_2}{V_1 - V_2}\right)X = 27.56\,\text{m}. \tag{21}$$

The error in pile length without correction is 3.7%. The error in the corrected pile length is 2.07%. It can be seen that the corrected test results could reflect the true pile length more accurately.

6. Conclusions

Based on the above theoretical analysis and the results of the finite element model validation, the following useful conclusions can be obtained:

In the process of fitting a straight line from the measured point data, the fitted data points for straight line L_1 should be selected close to the bottom of the pile, and the fitted data points for straight line L_2 should be selected at the bottom of the side hole. Such a selection method will maximise the theoretical assumptions of the straight line intersection method for determining the depth of the pile bottom in order to improve the accuracy of the judgement.

The larger the length-diameter ratio of the pile and the smaller the distance between the side hole and the pile, the more accurate the test results. The inclination angle of the side hole has a greater effect on the distribution of data points in straight line L_1 and has almost no effect on the distribution of data points in straight line L_2.

Method 1, the straight line intersection method, yields the pile bottom depth value that is greater than the actual pile bottom depth value, so the correction factor needs to be introduced to correct the result. Method 2, the translational straight line method, produces a pile bottom depth value that is theoretically consistent with the actual pile bottom depth value. When the correction factor about the inclination of the side hole is introduced according to actual needs, the corrected test results can be better improve the accuracy of the test.

Data Availability

The data used to support the findings of this study are available from the corresponding author upon request.

Conflicts of Interest

The authors declare that there are no conflicts of interest.

Authors' Contributions

Data curation was carried out by C.L. and C.Z.; validation was performed by B.A. and B.Z.; formal analysis was performed by T.Z.; software was the responsibility of X.T.; writing original draft was carried out by C.Z. and L.R.; writing, reviewing, and editing were performed by L.R. All authors have read and agreed to the published version of the manuscript.

Acknowledgments

This research was funded by the Science and Technology Research Project of Jiangxi Provincial Department of Education in 2021 (No. GJJ211643).

References

[1] G. Militano and R. K. N. D. Rajapakse, "Dynamic response of a pile in a multi-layered soil to transient torsional and axial loading," *Géotechnique*, vol. 49, no. 1, pp. 91–109, 1999.

[2] A. G. Davis, "Nondestructive evaluation of existing deep foundations," *Journal of Performance of Constructed Facilities*, vol. 9, no. 1, pp. 57–74, 1995.

[3] L. D. Olson, F. Jalinoos, and M. F. Aouad, "Determination of unknown subsurface bridge foundations," *Report submitted to NCHRP, Transportation Research Board, National Research Council*, pp. 129–148, 1995.

[4] J. Tang and D. Huang, "Study on the quality of cement mixing pile detected by side-hole transmission wave method," *China Municipal Engineering*, vol. 6, pp. 83–85, 2006.

[5] S. Liao, J. Tong, C. Chen, and T. Wu, "Numerical simulation and experimental study of parallel seismic test for piles," *International Journal of Solids and Structures*, vol. 43, no. 7-8, pp. 2279–2298, 2006.

[6] D. Huang and L. Chen, "3D finite element analysis of parallel seismic method for integrity of cemented soil columns," *Journal of Shanghai Jiaotong University*, vol. 41, no. 6, pp. 960–964, 2007.

[7] D. Huang and L. Chen, "3D finite element analysis of parallel seismic tests for integrity of piles of existing structures," *Rock and Soil Mechanics*, vol. 29, no. 6, pp. 1569–1574, 2008.

[8] L. Chen and R. Zhao, "On determination of pile length with parallel seismic testing for existing structure," *Chinses Journal of Underground Space and Engineering*, vol. 6, pp. 157–161, 2010.

[9] Y. Du, L. Chen, Y. Ma, and Y. Yang, "Determination of pile length using parallel seismic testing with FEM simulation," *Journal of Disaster Prevention and Mitigation Engineering*, vol. 32, pp. 731–736, 2012.

[10] J. Zhang, L. Zhang, L. Chen, and Y. Ma, "Effect of exciting mode on detection of existing pile with parallel seismic method," *Journal of Disaster Prevention and Mitigation Engineering*, vol. 35, pp. 180–185, 2015.

[11] Z. Jing-Yi, C. Long-Zhu, and Z. Jinying, "Theoretical basis and numerical simulation of parallel seismic test for existing piles using flexural wave," *Soil Dynamics and Earthquake Engineering*, vol. 84, pp. 13–21, 2016.

[12] J. Y. Zhang and L. Z. Chen, "Selection of pile testing signals for parallel seismic test," *Advanced Materials Research*, vol. 368-373, pp. 2045–2049, 2011.

[13] Y. Du, C. Song, L. Chen, and J. Yang, "PS wave based parallel seismic test for pile length assessment," *Soils and Foundations*, vol. 56, no. 3, pp. 440–448, 2016.

[14] S. Rashidyan, T. T. Ng, and A. Maji, "Exploratory study of nondestructive parallel seismic testing challenges in estimating the depth of unknown wood bridge foundations," *Journal of*

Performance of Constructed Facilities, vol. 34, no. 3, p. 34, 2020.

[15] S. Rashidyan, A. Maji, and T. Ng, "Performance of nondestructive parallel seismic testing method in determining depth of shallow foundations," *Journal of Performance of Constructed Facilities*, vol. 33, no. 2, p. 6019001, 2019.

[16] Y. Huang and S. Ni, "Experimental study for the evaluation of stress wave approaches on a group pile foundation," *NDT and E International*, vol. 47, pp. 134–143, 2012.

[17] B. Yuan, Z. Li, Z. Zhao, H. Ni, Z. Su, and Z. Li, "Experimental study of displacement field of layered soils surrounding laterally loaded pile based on transparent soil," *Journal of Soils and Sediments*, vol. 21, no. 9, pp. 1–12, 2021.

[18] B. Bai, R. Zhou, G. Cai, W. Hu, and G. Yang, "Coupled thermo-hydro-mechanical mechanism in view of the soil particle rearrangement of granular thermodynamics," *Computers and Geotechnics*, vol. 137, article 104272, 2021.

[19] B. Yuan, Z. Li, Y. Chen et al., "Mechanical and microstructural properties of recycling granite residual soil reinforced with glass fiber and liquid-modified polyvinyl alcohol polymer," *Chemosphere*, vol. 286, no. P1, article 131652, 2022.

[20] B. Bai, Y. Wang, D. Rao, and F. Bai, "The effective thermal conductivity of unsaturated porous media deduced by pore-scale SPH simulation," *Frontiers in Earth Science*, no. article 943853, 2022.

[21] B. Yuan, Z. Li, W. Chen et al., "Influence of groundwater depth on pile–soil mechanical properties and fractal characteristics under cyclic loading," *Fractal and Fractional*, vol. 6, no. 4, pp. 198–198, 2022.

[22] C. Lin, L. Rao, C. L. Zhang et al., "A study of dynamic loading and unloading damage of fiber-reinforced concrete under confining pressure," *Geofluids*, vol. 2022, Article ID 7751265, 10 pages, 2002.

[23] J. Lifu, "Research on the influence of pile foundation construction of a bridge on adjacent subway tunnels based on ABAQUS," *Highway Engineering*, vol. 45, no. 4, pp. 147–151, 2020.